

## Article

# Applied Intelligent Grey Wolf Optimizer (IGWO) to Improve the Performance of CI Engine Running on Emulsion Diesel Fuel Blends

Hussein Alahmer <sup>1,\*</sup>, Ali Alahmer <sup>2,3,\*</sup>, Razan Alkhazaleh <sup>2</sup>, Mohammad Alrbai <sup>4</sup> and Malik I. Alamayreh <sup>5</sup> 

<sup>1</sup> Department of Automated Systems, Faculty of Artificial Intelligence, Al-Balqa Applied University, Al-Salt 19117, Jordan

<sup>2</sup> Department of Industrial and Systems Engineering, Auburn University, Auburn, AL 36849, USA

<sup>3</sup> Department of Mechanical Engineering, Faculty of Engineering, Tafila Technical University, Tafila 66110, Jordan

<sup>4</sup> Department of Mechanical Engineering, School of Engineering, University of Jordan, Amman 11942, Jordan

<sup>5</sup> Department of Alternative Energy Technology, Faculty of Engineering and Technology, Al-Zaytoonah University, Amman 11733, Jordan

\* Correspondence: dr.halahmer@bau.edu.jo (H.A.); aza0300@auburn.edu (A.A.)

**Abstract:** Water-in-diesel (W/D) emulsion fuel is a potential alternative fuel that can simultaneously lower NO<sub>x</sub> exhaust emissions and improve combustion efficiency. Additionally, there are no additional costs or engine modifications required when using W/D emulsion fuel. The proportion of water added and engine speed is crucial factors influencing engine behavior. This study aims to examine the impact of the W/D emulsion diesel fuel on engine performance and NO<sub>x</sub> pollutant emissions using a compression ignition (CI) engine. The emulsion fuel had water content ranging from 0 to 30% with a 5% increment, and 2% surfactant was employed. The tests were performed at speeds ranging from 1000 to 3000 rpm. All W/D emulsion fuel was compared to a standard of pure diesel in all tests. A four-cylinder, four-stroke, water-cooled, direct-injection diesel engine test bed was used for the experiments. The performance and exhaust emissions of the diesel engine were measured at full load and various engine speeds using a dynamometer and an exhaust gas analyzer, respectively. The second purpose of this study is to illustrate the application of two optimizers, grey wolf optimizer (GWO) and intelligent grey wolf optimizer (IGWO), along with using multivariate polynomial regression (MPR) to identify the optimum (W/D) emulsion blend percentage and engine speed to enhance the performance, reduce fuel consumption, and reduce NO<sub>x</sub> exhaust emissions of a diesel engine operating. The engine speed and proportion of water in the fuel mixture were the independent variables (inputs), while brake power (BP), brake thermal efficiency (BTE), brake-specific fuel consumption (BSFC), and NO<sub>x</sub> were the dependent variables (outcomes). It was experimentally observed that utilizing emulsified gasoline generally enhances engine performance and decreases emissions in general. Experimentally, at 5% water content and 2000 rpm, the BSFC has a minimal value of 0.258 kJ/kW·h. Under the same conditions, the maximum BP of 11.6 kW and BTE of 32.8% were achieved. According to the IGWO process findings, adding 9% water to diesel fuel and running the engine at a speed of 1998 rpm produced the highest BP (11.2 kW) and BTE (33.3%) and the lowest BSFC (0.259 kg/kW·h) and reduced NO<sub>x</sub> by 14.3% compared with the CI engine powered by pure diesel. The accuracy of the model is high, as indicated by a correlation coefficient R<sup>2</sup> exceeding 0.97 and a mean absolute error (MAE) less than 0.04. In terms of the optimizer, the IGWO performs better than GWO in determining the optimal water addition and engine speed. This is attributed to the IGWO has excellent exploratory capability in the early stages of searching.



**Citation:** Alahmer, H.; Alahmer, A.; Alkhazaleh, R.; Alrbai, M.; Alamayreh, M.I. Applied Intelligent Grey Wolf Optimizer (IGWO) to Improve the Performance of CI Engine Running on Emulsion Diesel Fuel Blends. *Fuels* **2023**, *4*, 35–57. <https://doi.org/10.3390/fuels4010004>

Received: 15 November 2022

Revised: 22 December 2022

Accepted: 10 January 2023

Published: 31 January 2023



**Copyright:** © 2023 by the authors. Licensee MDPI, Basel, Switzerland. This article is an open access article distributed under the terms and conditions of the Creative Commons Attribution (CC BY) license (<https://creativecommons.org/licenses/by/4.0/>).

**Keywords:** water/diesel emulsion; optimization; diesel engine; regression; exhaust emission; engine performance

## 1. Introduction

Improved combustion efficiency, superior durability, and higher reliability are desirable characteristics of compression ignition (CI) engines over spark ignition (SI) engines, which can also prevail in the power and transportation generating sectors [1]. The pollutants produced by CI engines, particularly NO<sub>x</sub>, are hazardous to the environment and public health. Numerous attempts have been performed to enhance fuel quality using various methods to minimize exhaust and acoustic emissions while improving engine performance [2,3]. Consequently, numerous studies have advocated using water-in-diesel (W/D) fuel because it improves the thermal efficiency of CI engines and reduces exhaust emissions with no extra cost or engine modification. Three methods have been developed for using water in CI engines: direct water injection into the cylinder, water injection into the inlet manifold, and W/D emulsion fuel [4]. The W/D technique is more intriguing because it can reduce harmful exhaust emissions without modifying the engines [5]. It was reported that using W/D fuels reduced NO<sub>x</sub> emissions and improved thermal engine performance without substantially increasing specific fuel consumption (SFC). However, W/D combustion can elevate unburn hydrocarbon (UHC) emissions due to the high latent heat of the vaporization of water.

In order to prepare two-phase emulsions of oil-in-water or water-in-oil, a surfactant must be added to reduce the oil and water surface tension and enhances their superficial contact areas [6]. The surfactant suspended the water droplets in the W/D emulsion. Therefore, water does not directly contact the engine surfaces. Additives are used to preserve the emulsion, improve the lubricity, prevent corrosion, and prevent freezing [7]. Syafiq et al. [8] employed a W/D emulsion in the volumetric range of 5–15% fuels combined with surfactant Span 80 and Tween 80 to address engine performance. They stated that increasing the water content of an emulsion by up to 15% increased the diesel engine's capability to burn fuel efficiently. Additionally, when the water content increased, the ignition delay time (IDT) and peak pressure (P.P.) increased, whereas the BP decreased. Tan et al. [9] affirmed that utilizing emulsion fuels that include a blend of Span 80 and Tween 80 causes BP and brake torque (BT) to be lower than when using pure diesel fuel.

### 1.1. Literature Review on Emulsion Diesel Fuel

Several studies examined the impact of introducing water into diesel fuel and showed the effect on CI engine combustion, performance, and exhaust emissions. Ghojel et al. [10] studied the impact of W/D emulsion fuel with varying volumetric water contents. The water added to the fuel significantly affected the IDT. Sharma et al. [11] examined the performance of a single-cylinder CI engine powered by a W/D emulsion containing (5–25%) % water. At all load ratios, increasing the water percentage of the emulsion resulted in minimal improvement in the BTE. Seifi et al. [12] investigated engine performance and noise emissions using W/D emulsion fuel containing 2–10% volumetric water. According to these findings, adding 2% water to pure diesel fuel boosted BP while displaying equivalent torque and noise emission levels. Azimi et al. [13] examined CI engine performance and emissions using 0–10% W/D emulsion fuels. They showed that W/D emulsion containing 2% water enhanced the CI engine performance and reduced exhaust pollutants. Kumar et al. [14] investigated CI engine performance and emissions utilizing a 10% W/D emulsion fuel at varying injection angles. This study indicated that emulsion fuel enhanced brake thermal efficiency (BTE). Furthermore, the W/D emulsion fuel significantly reduced NO<sub>x</sub>, CO, and UHC due to the improved combustion efficiency and decreased peak flame temperature. Syu et al. [15] studied the influence of W/D emulsion fuels on diesel engine behavior. According to the experimental results, the BTE improved by approximately 1.2–19.9%.

Vellaiyan et al. [16] critically assessed the use of W/D emulsified fuels. They examined the characteristics, stability, and impact of nano additions on the performance and exhaust emissions of CI engines. According to Attia et al. [17], smaller droplets in a W/D emulsion fuel have a more obvious effect on engine performance. Pamminger et al. [18] evaluated the influence of dilution by exhaust gas recirculation (EGR) and port-injected water on

the performance parameters of the fuel operation. The BTE was lowered for diesel and gasoline fuels using port-injected water and EGR dilution. Korakianitis et al. [19] explored a hydrogen–biodiesel dual-fuel engine. Compared to the rapeseed methyl ester (RME), the W/D fuel enhanced the BTE at higher engine speeds. At 750 r/min, 5% and 10% emulsified fuels decreased NO<sub>x</sub>.

### 1.2. Literature Review on Optimization Methods for Diesel Engine Behavior

In order to evade budgetary restrictions and time-consuming trials, scholars have used a variety of modeling and optimization approaches, such as artificial intelligence; fuzzy logic modeling; and meta-heuristic algorithm optimization, such as particle swarm optimization (PSO), whale optimization algorithm (WOA), artificial bee colony (ABC), etc. [20–24]. An effort was undertaken to develop a reliable water–diesel emulsion with optimum formulation and process parameters, as well as to analyze the performance and emission characteristics of CI engines employing different optimization strategies. Kumar et al. [21] generated 54 samples with different W/D ratios, surfactant concentrations, and stirring speeds. After 24 and 48 h of emulsification, water separation was measured. The collected data were utilized in the artificial neural network (ANN)–particle swarm optimization (PSO) approach to determine the best parameters for producing W/D emulsions for CI engine testing conditions. The best settings were a 20% W/D ratio, 0.9% surfactant, and 2200 rpm stirring speed for a 14.33% water separation in one day with a 6.54% variation. Vellaiyan and Amirthagadeswaran [25] employed Taguchi-Gree to optimize W/D content. The optimal ratios for W/D fuel were reported to be 1% surfactant content, 5000 rpm stirring speed, and 5% added water. However, the stirring speed and mixing time (30 min.) was too high for the 5% water emulsion. Lin et al. [26] stated that the Taguchi technique could not locate the best settings with continuous control parameters. Ahmad and Janahiraman [27] demonstrated that PSO outperformed the Taguchi technique and genetic algorithm (GA) in identifying optimum control settings.

### 1.3. Research Gap, Objectives, and Novelty

The use of a W/D emulsion fuel is an option for improving engine performance and reducing nitrogen oxide (NO<sub>x</sub>) emissions from CI engines. However, due to the influence of the water content in the diesel fuel, several other parameters, such as BP, were slightly lower. In other words, maintaining harmony between engine performance and emissions has always been a significant challenge in the automotive industry. Few studies have focused on determining the optimum water percentage added to form a W/D emulsion diesel fuel. Fuel blends with different proportions are repetitive and costly. Finding the best mixture to increase the CI engine performance while simultaneously reducing exhaust pollution requires conducting tests for all test setups. Alternatively, this challenge could be solved using various optimization techniques, enabling the identification of the appropriate blending percentage, producing the highest BP and BTE and the lowest BSFC and NO<sub>x</sub> emissions. Depending on the situation, researchers have used a variety of optimization methodologies to enhance the input parameters to decrease or increase the response [28]. It is worth noting that the IGOW can anticipate unquantified data in data analysis and find the best solution. In general, IGOW can be employed to maximize the engine behavior powered by different fuels, loads, ignition timing, compression ratios, etc. IGWO optimization can offer the optimum option for better combustion and reduced emissions in internal combustion engines. When compared to the GOW optimizer, the experimental design of IGWO can obtain better results with fewer tests and effort.

This study examines the behavior of diesel engines operating on 0–30% water addition mixtures under full load conditions and at different engine speeds. In addition, the quantity of water added to diesel fuel and engine speed was optimized for optimum engine performance and reduced NO<sub>x</sub> exhaust emissions. The main contribution of this study is to propose a novel framework consisting of two stages, as follows: the first stage employs the MPR model in order to evaluate the nonlinear relationship between the dependent

and independent variables. In this work, engine speed and the percentage of water in the fuel mixture were the independent variables. The four dependent variables were BP, BTE, BSFC, and NO<sub>x</sub>. The second stage is applying and comparing two optimizers, IGWO and GWO, which were utilized to locate the ideal conditions for the water % in the fuel mixture and engine speed to enhance engine performance, reduce fuel consumption, and reduce NO<sub>x</sub> exhaust emissions of a diesel engine. According to the author's knowledge, there is no current literature on using the above-mentioned technique to improve diesel engine operation.

## 2. Experimental Methodology

The W/D emulsion is composed of a mixture of diesel fuel and regular tap water. W/D emulsion mixtures were developed with varying water percentages (5–30% with 5% augmentation) by volume. The surfactant of polysorbate 20, known as Tween 20, was employed at 2% by volume to stabilize the W/D emulsions. The W/D emulsion fuels were developed using a homogenizer emulsification apparatus in two phases. Tween 20 surfactant was combined with diesel in the first stage. The pre-emulsions were then formed by gradually adding specific quantities of water to a combination of surfactant and diesel fuel while constantly swirling at 800 rpm for 5 min. In the second stage, the pre-emulsions were swirled at high speed at 5000 rpm for 20 min [29]. The 5% W/D emulsion fuel demonstrated the highest stability. The emulsion remained stable for at least 20 days without separation processes for all W/D emulsion fuel produced. Physical characteristics, such as fuel density, dynamic viscosity, and calorific value (C.V.), were measured for the synthesized W/D emulsion fuels. Pure diesel was utilized as a baseline for the comparison of all the W/D emulsion fuel blends.

In this study, a series of tests were performed on a four-stroke, water-cooled, four-cylinder, direct-injection CI engine. All the experimental tests were performed at the mechanical engineering laboratories of the University of Jordan. Table 1 lists the details of CI engine specifications. The CI engine was attached to a dynamometer to evaluate its performance. The dynamometer is a 400 V direct current (DC) machine, which is a compound wound, individually excited, and solely utilized for absorbing power. The highest allowed speed was 3000 rpm. However, the belt reduction drive allowed the engine to achieve a speed of 5000 rpm. Belt drives eliminate the requirement for flexible coupling to compensate for shaft misalignment and exhibit minimal friction and hysteresis losses. A steady torque of 80 N·m was maintained between 1500 and 3000 rpm. Two stops restricted the dynamometer. However, the torque arm should "float" between stops during operation. The test method was structured into the following steps: The CI engine was heated until it reached steady-state settings, and the lubricating oil temperature was kept between 80 and 90 °C for each trial. A brake load is applied, and the throttle is adjusted to its OWT. The data for BT, temperatures, engine speed, fuel weight, and air intake were then gathered and recorded. The above processes were performed for various W/D emulsion fuels. Before performing any tests, the CI engine and dynamometer were calibrated and set to their default parameters. All measurement data were recorded when the engine was stabilized. The tests were performed three times for each tested fuel, and the data average was considered.

**Table 1.** Technical data of automotive 30 test bed diesel engine.

Parameter	Diesel Engine Specifications
Type	Automotive 30 test bed
Bore × Stroke	72.25 × 88.18 mm
Number of cylinders	Four cylinders
Engine operation	Four strokes
Type of injection	Direct injection

**Table 1.** Technical data of automotive 30 test bed diesel engine.

Parameter	Diesel Engine Specifications
Type of injection	Direct injection
Air intake process	Naturally aspirated
Type of cooling	Water cooled
Swept volume	1450 cc
Compression ratio	21.5:1
Intake and exhaust valve diameter	34.51 × 28.49 mm
Connected rod length	155.8 mm
Dynamometer	400 V (nominal) DC machine

The NO<sub>x</sub> emissions were detected using a gas analyzer manufactured by Kane. It is essential to ensure that a 40–50 mm-diameter exhaust duct is supplied for the removal of exhaust gases to prevent unwanted backpressure [30]. The duct extends into a chamber for expansion or a silencer.

The uncertainty analysis was used to quantify the disparity between the actual and true values of a physical quantity. By using Equations (1) and (2), the percentage of uncertainty for different values such as BT, BTE, and BSFC was calculated.

$$\omega_R = \pm \sqrt{\left(\frac{\partial R}{\partial X_1} \omega_{X_1}\right)^2 + \left(\frac{\partial R}{\partial X_2} \omega_{X_2}\right)^2 + \left(\frac{\partial R}{\partial X_3} \omega_{X_3}\right)^2 + \dots + \left(\frac{\partial R}{\partial X_n} \omega_{X_n}\right)^2} \quad (1)$$

$$\text{Percentage Analysis} = \frac{\omega_R}{|R|} \times 100\% \quad (2)$$

where  $\omega_R$  is the uncertainty error,  $x$  is a variable, and  $\omega$  is the realistic error. The measured BP, BTE, and BSFC uncertainties were 2.2%, 2.4%, and 2.62%, respectively. This demonstrates the reliability of the results.

### 3. Modeling and Optimization

#### 3.1. Grey Wolf Optimization (GWO)

Mirjalili et al. [31] proposed GWO, which is a population-based optimization approach. The GOW is a swarm intelligence program inspired by the natural leadership structure and hunting behavior of grey wolves. Grey wolf populations were divided into four groups based on their significant tasks, which formed a four-level leadership hierarchy:  $\alpha$ ,  $\beta$ ,  $\delta$ , and  $\omega$ . The social hierarchy is illustrated in Figure 1. Alpha ( $\alpha$ ) indicates the group member with the highest dominance. The remaining subordinates are beta ( $\beta$ ) and delta ( $\delta$ ), which assist in maintaining order in the bulk of wolves in the hierarchy, known as omega wolves ( $\omega$ ).

GWO is classified into three phases: (A) encircling prey, (B) hunting prey, and (C) attacking prey, as detailed below.

#### Encircling prey

Grey wolves surround their prey when hunting, which may be described mathematically, as indicated in Equation (3).

$$X(t+1) = X_p(t) - A \times D \quad (3)$$

where

$$A = 2\alpha r_1 - \alpha \quad (4)$$

$$D = |C \times X_p(t) - X(t)| \quad (5)$$

$$C = 2r_2 \quad (6)$$



Figure 1. GWO social hierarchy.

The starting location of a wolf is given by  $X(t)$ , and its updated position surrounding the prey location at  $X_p(t)$  is computed by altering vectors  $A$  and  $C$ . The random vectors  $r_1$  and  $r_2$  of each  $(0, 1)$  enable the wolves to adjust the values of  $A$  and  $C$ . Equations (3)–(6) are utilized to control the initialization and updating of the GWO location  $(t + 1)$ .

**Hunting prey**

The  $\alpha$  wolf is regarded as the closest (optimum solution), followed by the  $\beta$  and  $\gamma$  wolves. The position of  $\omega$  fluctuates depending on the current optimal position. The final location, as it pertains to the positions of  $\alpha$ ,  $\beta$ , and  $\delta$  in the search space, is represented by Equations (7)–(9):

$$X(t + 1) = \frac{1}{3} \times (X_1 + X_2 + X_3) \tag{7}$$

where

$$X_1 = X_\alpha(t) - A_1 \times D_\alpha X_2 = X_\beta(t) - A_2 \times D_\beta X_3 = X_\delta(t) - A_3 \times D \tag{8}$$

and

$$D_\alpha = |C_1 \cdot X_\alpha - X| D_\beta = |C_2 \cdot X_\beta - X| D_\delta = |C_3 \cdot X_\delta - X| \tag{9}$$

**Attacking prey**

The last step of optimization occurs after identifying the prey’s location and the wolf’s approach to attack it. This strategy is mathematically expressed in Equation (10) by adjusting the parameter  $|\alpha|$ . The critical parameter of GWO,  $|\alpha|$ , which decreases linearly from 2 to 0 as the iteration progresses, is principally accountable for exploring and exploiting the search space.

$$\alpha = 2 - (t) \cdot \left( \frac{2}{T} \right) \tag{10}$$

The stages involved in GWO are as follows:

The lower and upper boundaries are utilized to generate random location vectors for the search agents.

Each agent’s fitness value was calculated using the population’s three wolf subgroups (alpha, beta, and delta). They used  $D_\alpha$ ,  $D_\beta$ , and  $D_\delta$  to change their location in order to grab the prey, as shown in Equation (9). Equation (8) was used to modify the location of the search agents.

In order to meet the termination conditions, the fitness assessment and update process procedures were repeated.

### 3.2. Intelligent Gray Wolf Optimizer (IGWO)

Saxena et al. [32] proposed IGWO to enhance the search capability of GWO. The IGWO is built on two conceptual structures: (i) a method for opposition-based learning (OBL) to boost both exploration and exploitation, and (ii) a truncated sinusoidal function for a variable  $|\alpha|$  to prevent its drop down linearly.

The OBL mechanism is based on the notion of opposing numbers and points to improve the convergence of population-based algorithms [33]. Regarding extreme points, the opposite number represents the mirror point of the solution. They represent the lower limit (LL) of the search space, the upper limit (UL), and the center, as indicated by Equation (11).

$$\chi_d^o = LL_d + UL_d - \chi_d \quad (11)$$

where point  $P (X_1, X_1, \dots, X_d)$ , the opposing point is  $P (X_1^o, X_2^o, \dots, X_d^o)$ , and  $d$  is the search space dimension.

In IGWO, half of the population is employed to create search agent positions randomly, whereas the other half is used for the remaining positions. As illustrated in Equation (12), the truncated sinusoidal function represented by parameter  $|\alpha|$  is employed to regulate the movement of the wolf.

$$\alpha = 2 \times \left( 1 - \sin^2 \frac{\varnothing}{2} \right) \quad (12)$$

where

$$\varnothing = \pi \times \frac{\text{Current iteration}}{\text{Max iteration}} \quad (13)$$

The Pseudocode of the optimization method is displayed in Figure 2.

```

Initialize Grey wolf population:  $X_i$  ( $i=1,2,\dots,n$ )
Assign  $t_{MAX}$ = a total of all iterations
Calculate the fitness value of each agent
Assign grey wolf population based on fitness values ( $\alpha$ ,  $\beta$  and  $\Delta$ )
While  $t < t_{MAX}$ :
    For each  $\vec{X}_i$  in  $\vec{X}$ :
        Update position of each wolf  $\vec{X}_i$ 
    End For
    Find the fitness of all population
    If  $\vec{X}_i$  improves Then
        Map a new location and move it there.
    End If
    Update alpha, beta, and delta
End while
Return alpha as the best solution
  
```

**Figure 2.** The Pseudocode of the optimization method.

Figure 3 depicts the flowchart of the intelligent gray wolf optimizer. The best, second-best, and third-best solutions are represented by  $\alpha$ ,  $\beta$ , and  $\Delta$  wolves, respectively. Each wolf's position is determined by the approximate location of the prey. Finally,  $\alpha$  is returned as the best response. A schematic representation of the experimental approach in combination with an optimization technique is illustrated in Figure 4.

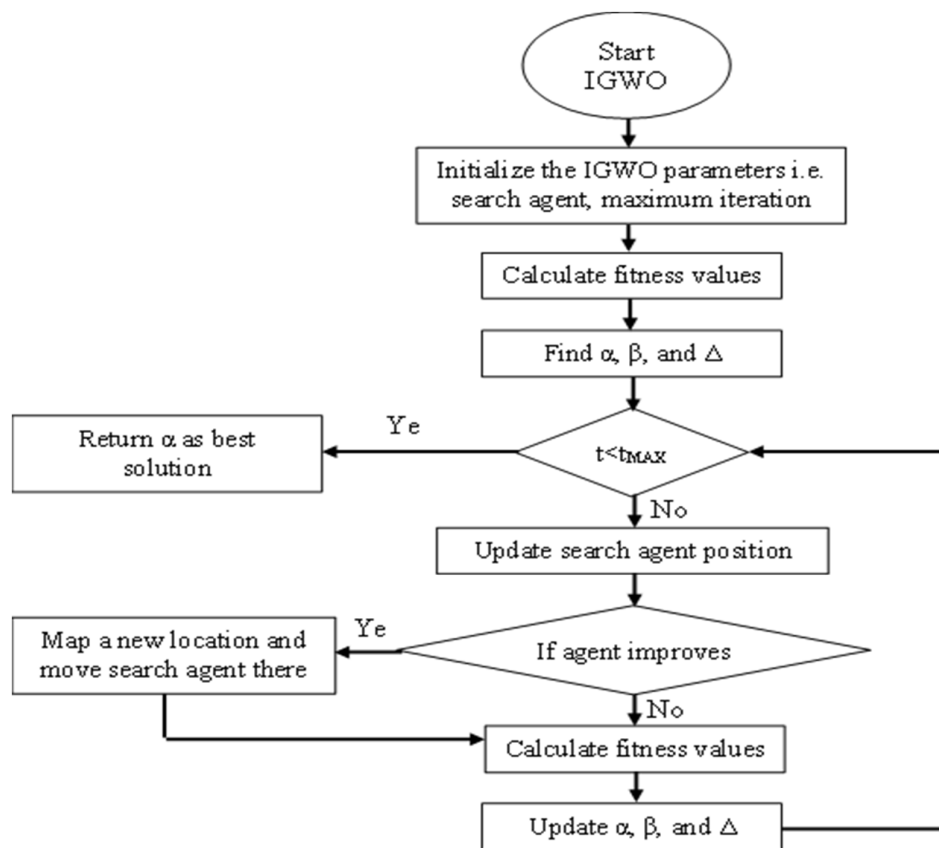


Figure 3. Flow chart of the IGWO approach process.

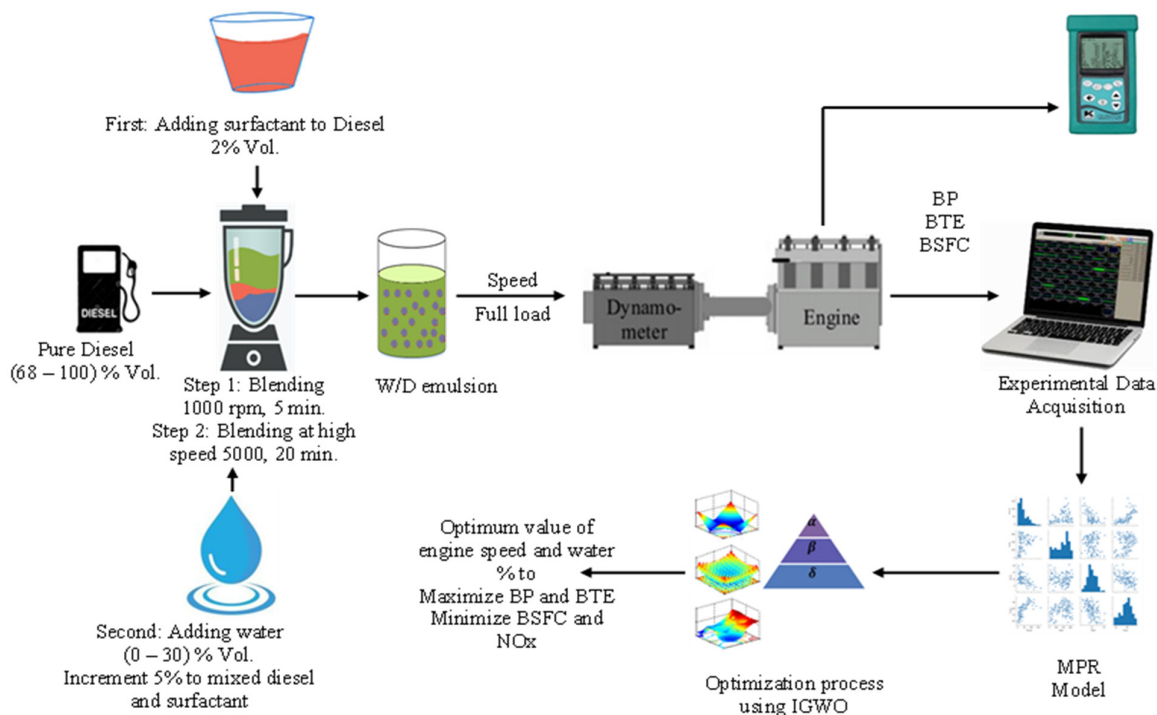


Figure 4. A schematic portrayal of the experimental strategy combined with an optimization method.

## 4. Results and Discussion

### 4.1. Experimental Analysis

Figures 5–7 demonstrate the physical characteristics of diesel and W/D emulsion fuels, such as fuel density, fuel dynamic viscosity, and fuel calorific heat (C.V.), with varying water percentages, respectively. Figure 5 indicates that the density of the W/D emulsion increased as the water quantity in the W/D emulsion blend increased. This is because of the higher water compared with pure diesel fuel. Figure 6 displays that the viscosity of the W/D emulsion increases with percentage water addition until a value of 43 centipoises at 15% water and subsequently drops. However, boosting the dynamic viscosity of W/D emulsions leads to an advanced injection time in particular injection systems. The viscosity of the W/D emulsion increased due to the formation of increasingly complex micellar structures, indicating the presence of water in oil under these conditions. Furthermore, a boost in the water addition to W/D emulsion fuel improves the interaction of water droplets and enhances the viscosity of fuels. The phase transitions to oil-in-water, and the viscosity reduces when more water is added. The high proportion of water added to W/D emulsion fuels results in poor atomization of droplets within the combustion chamber (C.C.). Figure 7 reveals that the calorific value of a W/D emulsion decreases with increasing water quantity. This is because of a phenomenon called heat sink (HS). When HS is formed, the water content of the inner phase soaks up some of the heat emitted by burning, thus lowering the heating value. In addition, because of the endothermic reaction of water. This behavior is consistent with the Dryer study [34].

Figures 8 and 9 show the BP generated by the CI engine utilizing the W/D emulsion and pure diesel fuels at varying speeds. As indicated, the developed BP is at its maximum when the CI engine is fueled by a 5% W/D emulsion and runs at a realistic speed. When the water percentage in the W/D exceeded 5%, the amount of BP generated dropped. The slight reduction in BP is attributable to the W/D fuel with a lesser C.V. than that of pure diesel fuel, releasing a small quantity of heat during combustion. However, a slight decrease in BP can be accepted when weighed against the enormous reduction in emissions achieved by utilizing W/D. This matches the findings of Hoseini et al. [35], Fahd et al. [36], and Okumuş et al. [37]. They observed that adding water to diesel increased the IDT. Because of the longer IDT during the compression stroke, the W/D emulsion fuels require less compression work than pure diesel fuel, representing negative work. This contributes to achieving a higher P.P. after the top dead center (TDC) to generate more BP during the power stroke. Moreover, as the IDT increased, more fuel was provided (via evaporation and mixing) for chemical reactions. This boosts the amount of fuel used and the rate at which heat is released during premixed combustion. Consequently, combustion was enhanced, and the combustion efficiency was improved. In addition, it is discernible that the impact of water addition intensifies at high speeds (the line slope in Figure 9 increases with velocity). Table 2 demonstrates the average changes in BP for CI engines driven by various percentages of W/D emulsion fuel against pure diesel fuel. This result is consistent with the findings of Nadeem et al. [38], Selim and Ghannam [39], and Yang et al. [40]. They observed no substantial variation in engine power when emulsified fuels were used under typical operating conditions. In contrast, the disparity in the generated BP is more pronounced at high velocities. According to several other tests, 20% water in the emulsion fuel provides the best engine performance [38]. Others observed that emulsions with 15–25% water might provide the best engine performance and fuel economy. Although the variation in water % might affect engine performance and emissions, it cannot be the sole reason. Many additional aspects that must be examined include the influence of fuel volatility, injection timing, test load, engine compression ratio, surfactant type, environmental conditions such as ambient temperature and pressure, and engine speed [39,41].

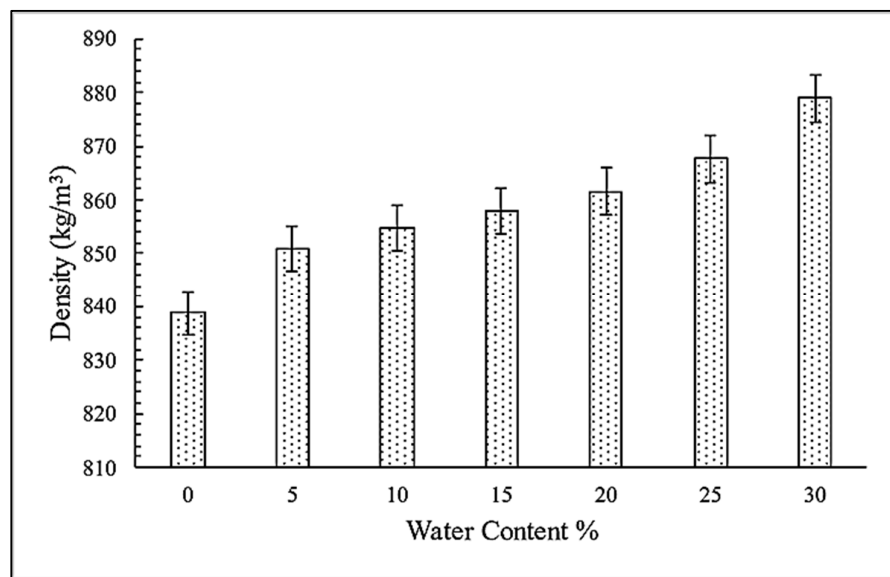


Figure 5. The density of different blends of the (W/D) fuel.

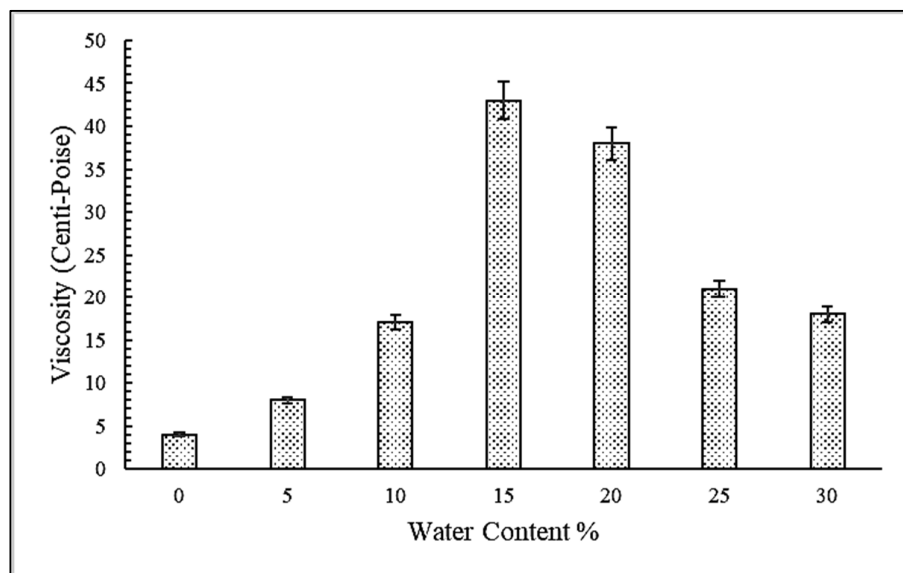


Figure 6. The viscosity of different blends of the (W/D) fuel.

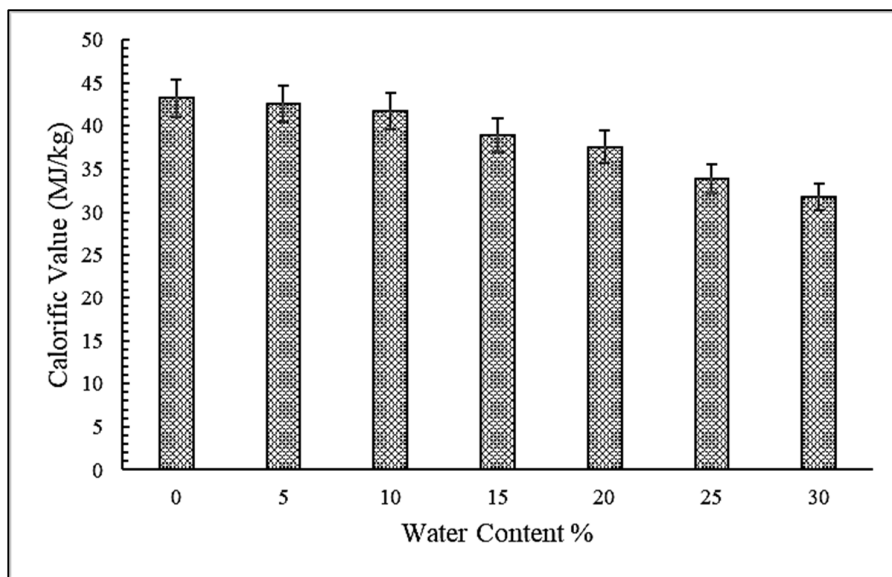


Figure 7. The calorific value (MJ/kg) of different blends of the (W/D) fuel.

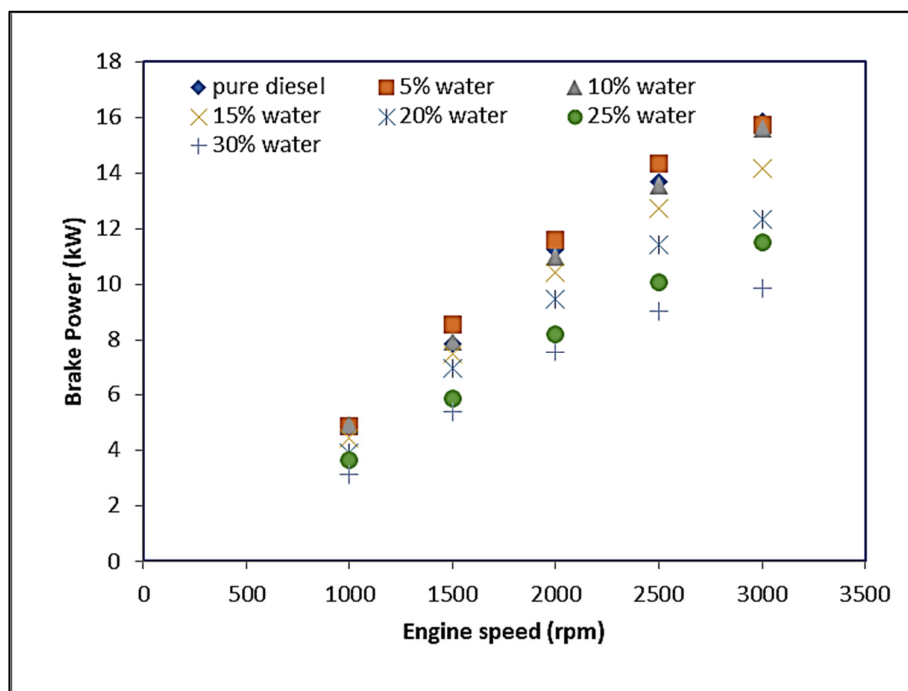
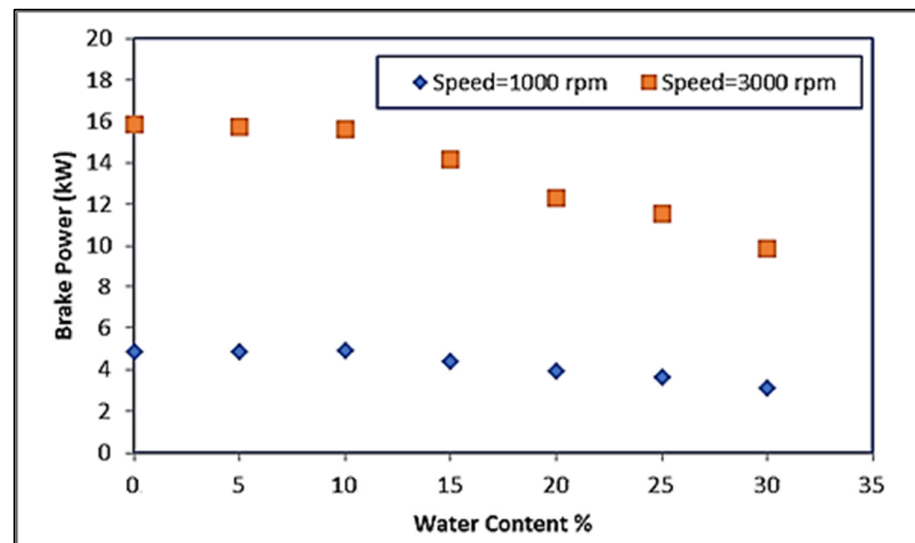


Figure 8. The fluctuation of BP (kW) as a function of rotation speed and water concentration.

Table 2. The average changes in BP, BSFC, BTE, and NOx for CI engines driven by various percentages of W/D emulsion fuel against pure diesel fuel.

Indicator	Water Addition					
	5%	10%	15%	20%	25%	30%
BP	3.00%	−0.90%	−7.90%	−17.64%	−26.43%	−34.61%
BSFC	−6.34%	−3.55%	6.34%	19.50%	27.82%	44.30%
BTE	7.94%	5.60%	2.81%	−5.06%	−3.65%	−8.35%
NOx	−3.22%	−9.60%	−20.42%	−53.40%	−64.38%	−67.14%



**Figure 9.** The fluctuation of BP (kW) as a function of water concentration and two constant engine speeds, 1000 and 3000 rpm.

Figure 10 depicts the BSFC of the CI engine while utilizing the W/D emulsion and pure diesel at variable speeds. Figure 10 shows that the BSFC was lowest at 2000 rpm and 5% water addition. Furthermore, reducing the engine speed produces a reduction in the BSFC until it arrives at its lowest value; after that, it rises. This is because, at low-speed rates, energy loss to the C.C. walls is proportionally higher than that at high speeds, subsequent in lower combustion efficiency. Consequently, more fuel consumption per unit of power is required. At high rotational engine speeds, the friction power shoots up, causing a slower power increase than that of fuel consumption. Increasing the water concentration enhances the BSFC at high speeds while having less influence at low-speed values. The rationale for boosting the BSFC by raising the water addition is that an equivalent amount of water displaces a large quantity of diesel. This implies that less diesel fuel is included in each emulsion volume. Alahmer et al. [6,42] demonstrated that utilizing W/D diesel reduces SFC due to the following: (i) the micro-explosion phenomenon, (ii) a greater volume of air is drawn into the spray as a result of its spray momentum, (iii) greater fuel consumption in premixed combustion because of a longer IDT, (iv) a rise in the local excess air ratio due to the injection of water, (v) decreased cooling loss due to flame temperature reduction, (vi) inhibition of the dissociation rate, and (vii) increased combustion output gas as a result of water vapor. Abu-Zaid [43] observed that utilizing emulsion fuel improves the BSFC significantly. Vellaiyan and Amirthagadeswaran [44] observed a 7.2% decrease in BSFC compared to pure diesel when employing 10% water addition in W/D emulsion fuel. This could be related to improved fuel blending and water droplet micro-explosion. Other experiments found a small increase in BSFC when W/D emulsion fuel was used to power the CI engine [36]. Although the amount of diesel fuel in the emulsion is decreased to the same amount of water replaced, the C.V. of the emulsion is reduced. Table 2 displays the average changes in BSFC for CI engines driven by various percentages of W/D emulsion fuel against pure diesel fuel. Ghojel et al. [45] showed a 22–26% increment in BSFC using W/D emulsion fuel with 13% water addition compared to diesel fuel.

Figure 11 depicts the BTE of the CI engine powered by W/D fuels at various speeds. As shown, The BTE improves as the rotational engine speed increases until it arrives at the highest value, following the BTE starts to decrease. At low rotation engine speeds, increased heat losses occur because of the long available time. As the speed increased, the BP increased, which enhanced the BTE. However, higher rotational engine speeds are followed by fast-developing friction power and increased inertia of the mechanical components, resulting in a decreased BTE. The greatest improvement in BTE occurred when a 5% W/D emulsion was employed due to the increased BP. Furthermore, the combustion

efficiency is significantly improved when the ignition is delayed, which causes micro-explosions. The presence of water in the emulsion is the cause of the prolonged delay in igniting. Furthermore, the inclusion of water in fuel produces latent heat during the process of vaporization. Therefore, it reduces the rate at which the droplet's temperature rises. Consequently, the physical delay becomes longer. Simultaneously, the existence of water vapor decreases the fuel concentration, increasing the chemical delay. Both the chemical and physical delays raise the total IDT [46]. Increased IDT enables more diesel fuel to be physically prepared for combustion reaction by evaporation and mixing processes, resulting in a boost in the heat release rates and fuel consumption in the premixed process. As a result, more diesel fuel is utilized and consumed. These characteristics boost combustion behavior and its efficiency [42,47].

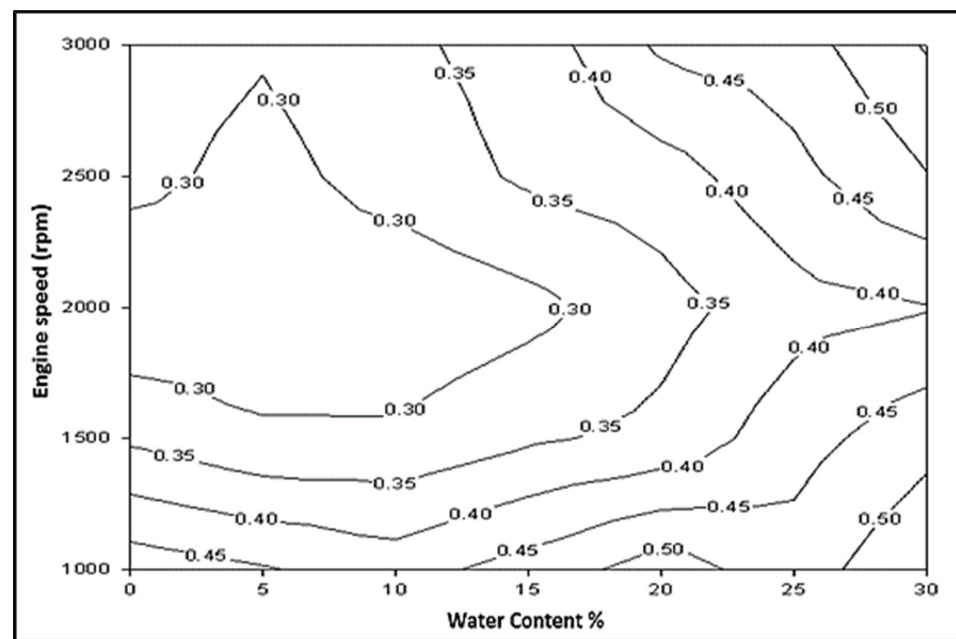


**Figure 10.** BSFC (kg/kW·h) for pure diesel and different water addition to diesel fuel.

Ithnin et al. [41] demonstrated that the greater the fuel dynamic viscosity of the W/D, the earlier it was prepared. However, this was accounted for by the increase in IDT caused by the water addition. As a result, the main chamber started heat discharge at the same time as pure fuel. Table 2 shows the average changes in BP for CI engines driven by various percentages of W/D emulsion fuel against pure diesel fuel.

Figure 12 depicts the fluctuation of NO<sub>x</sub> with the rotational engine speed for various W/D blends. Compared to the percentage of water added to diesel fuel, the engine speed has a minimal effect on NO<sub>x</sub> generation. When the W/D emulsion fuel was used, the CI engine emitted substantially less NO<sub>x</sub> than pure diesel. Most investigations coincided with our conclusion that utilizing the W/D emulsion fuel reduces NO<sub>x</sub> production significantly [17,48,49]. Table 2 illustrates the average changes in NO<sub>x</sub> for CI engines driven by various percentages of W/D emulsion fuel against pure diesel fuel. This is because the finely scattered water droplets of the emulsion generate a phenomenon known as a heat sink, which lowers the flame temperature. However, according to Jazair et al. [50], the decrease in NO<sub>x</sub> emitted from the CI engine is caused by the phase change in water to steam, which occurs in the C.C. and is an endothermic process that lowers the temperature within the cylinder. According to Dryer [34], the decrease in NO<sub>x</sub> is due to an increase in hydroxyl (OH) radical concentration caused by the water added to the diesel fuel. Selim and Elfeky [51] examined that the W/D emulsion fuel affected heat flow across the cylinder head and injector tip temperature, which affected NO<sub>x</sub> formation. The results showed that water lowers the metal temperature and heat flow through the cylinder head.

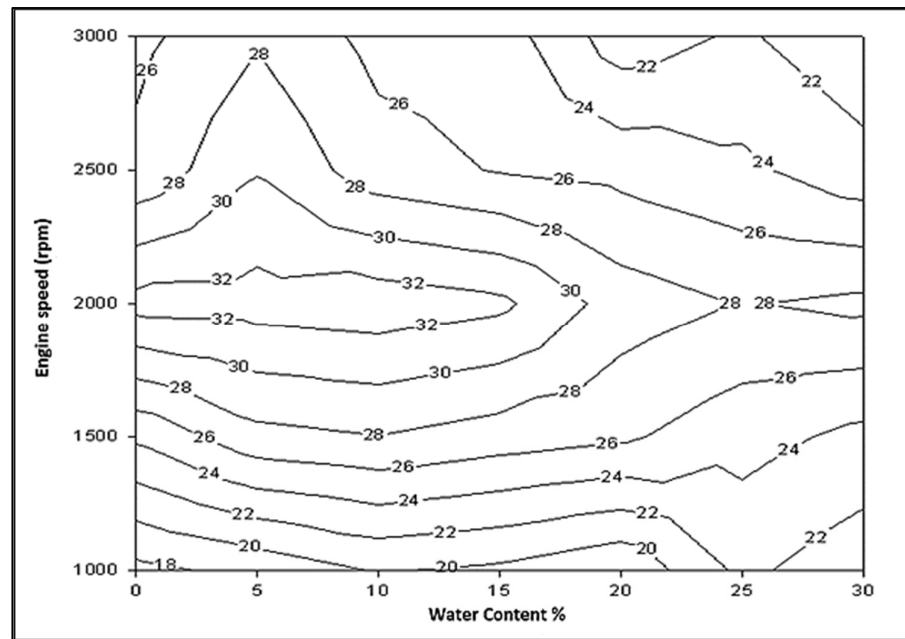


Figure 11. Brake thermal efficiency (%) for pure diesel and different water addition to diesel fuel.

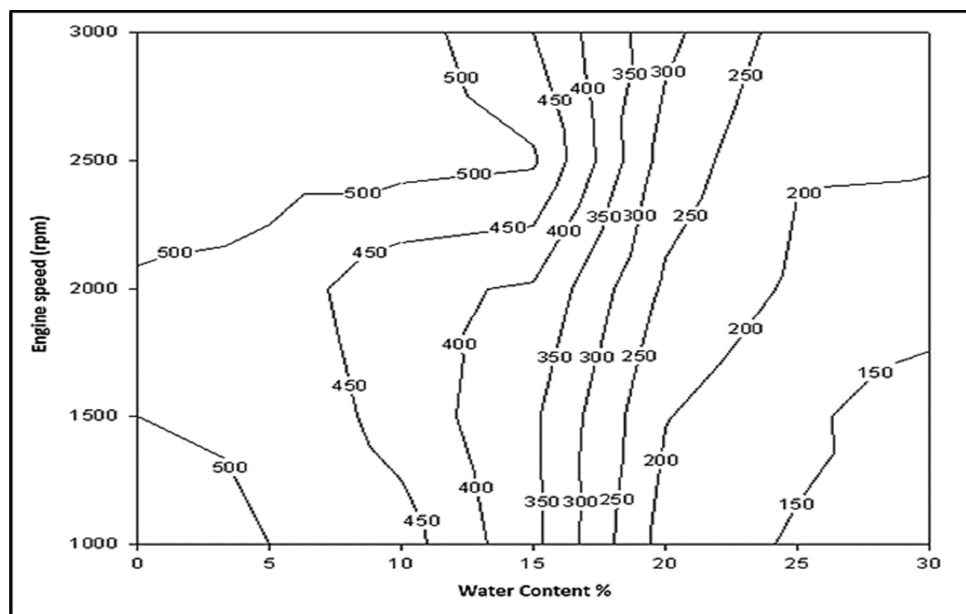


Figure 12. NOx (ppm) variation for pure diesel and different water addition to diesel fuel.

#### 4.2. Regression Model and Optimization Process

The trials were conducted using Python. The experiment included two stages. First, regression modeling was used to test the association between the response (engine performance and NOx exhaust emissions) and variables (engine speed and water addition percentage in the fuel mixture). Second, the IGWO approach maximizes the BTE and BP while minimizing the BSFC and NOx emissions.

##### 4.2.1. Fitting Regression Models

Regression is a method for inferring a relationship from the provided data in order to display the features of the dataset. This relationship can be used to perform a range of computations, such as estimating future values and establishing whether various variables are related.

Regression analysis consists of four steps: (i) identifying dependent and independent variables; (ii) using a scatter diagram between the dependent and independent variables, and the type of relationship between the variables can be determined, such as linear, parabolic, exponential, etc.; (iii) analysis via the computing of regression; and (iv) conducting an error analysis to determine whether the predicted model matches the actual data set.

There are several types of regression analysis, including (1) simple linear regression (SLR), as displayed in Equation (14), where the variables are linearly related; (2) polynomial regression (PR), as represented by Equation (15), the  $n$ th-order polynomial equation is employed to simulate nonlinearity between the response and the regressor variable; and (3) multivariate polynomial regression (MPR), as indicated by Equation (16), can be computed using several regressor variables [52].

$$y = \alpha + \beta_1x \tag{14}$$

$$y = \alpha + \beta_1x + \beta_2x^2 + \dots + \beta_{n-1}x^{n-1} + \beta_nx^n \tag{15}$$

$$y = \alpha + \beta_1x_1 + \beta_2x_2 + \beta_{11}x_1^2 + \beta_{22}x_2^2 + \beta_{12}x_1x_2 \tag{16}$$

where  $y$  is the dependent variable;  $x$ ,  $x_1$ , and  $x_2$  are the independent variables;  $\alpha$  is the intercept;  $\beta$  is the regression coefficient; and  $n$  is the polynomial degree.

Multivariate polynomial regression (MPR) framework was adopted in this study, as displayed in Figure 13. The rotational engine speed and percentage of water in the (W/D) mixture were independent variables. The engine effectiveness, including BP, BTE, and BSFC, and emissions of NOx were the dependent variables.

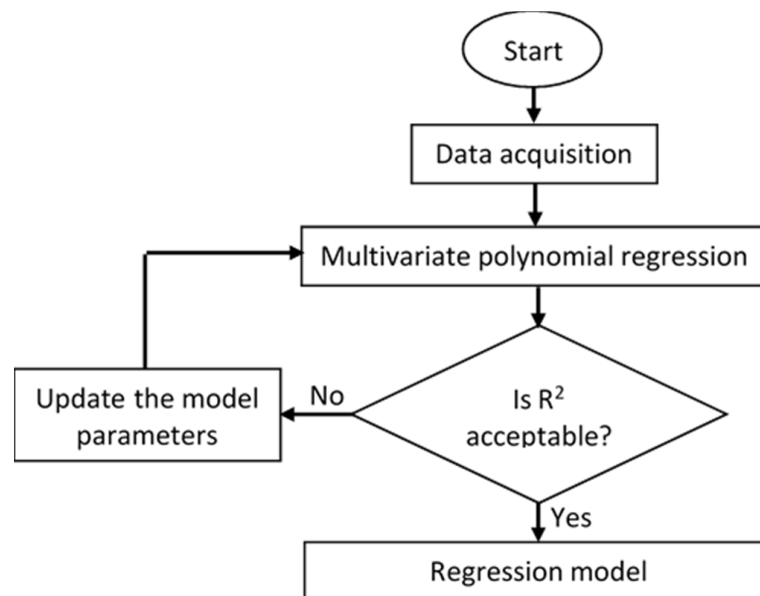


Figure 13. The MPR model flowchart.

According to the model assessment in Table 3, the mean absolute error (MAE) and decision coefficient ( $R^2$ ) can serve as indications of a model’s efficacy in regression prediction tasks.

Table 3. Multivariate polynomial regression evaluation.

Experiment	MAE	$R^2$
BP	0.0188	0.994
BTE	0.0398	0.977
BSFC	0.0219	0.983
NOx	0.0208	0.986

A visual portrayal was used to analyze the regression model. Consequently, the forecasting accuracy of the models was proven by plotting their predictions against the corresponding targets, as depicted in Figure 14. This indicates the closeness of the regression models to the input observations.

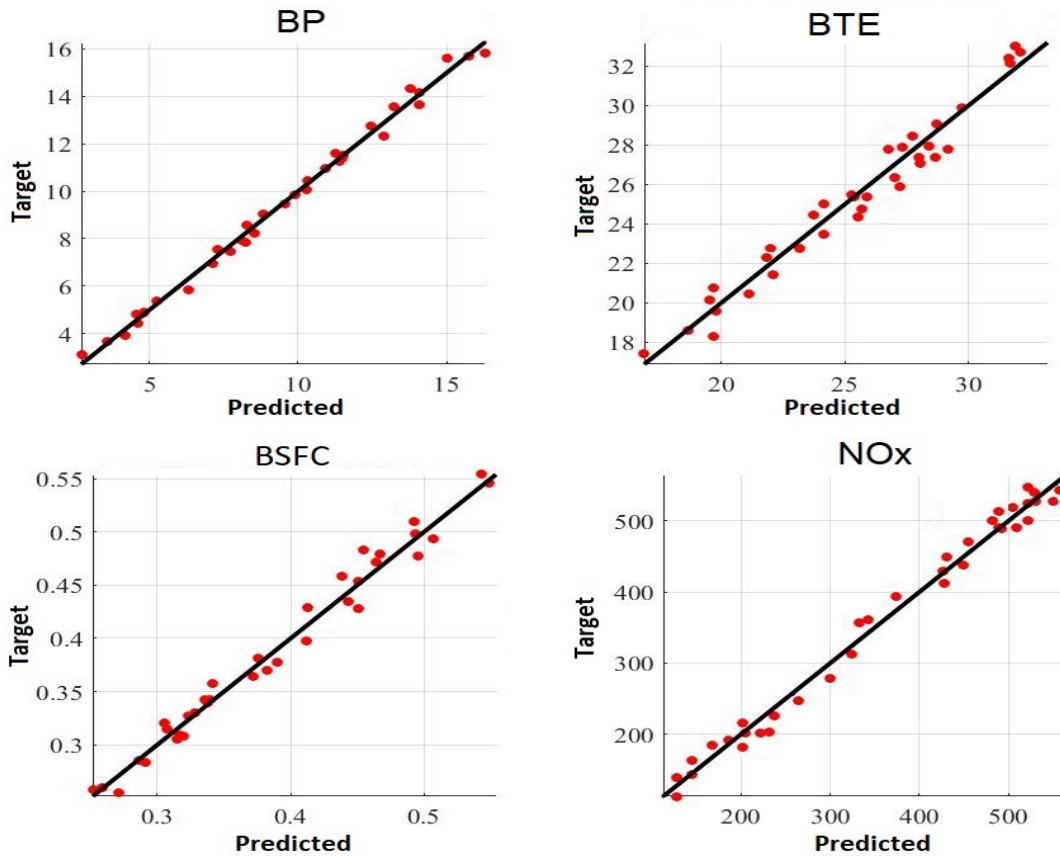


Figure 14. Regression model prediction precision.

4.2.2. IGWO Optimization

The tests were performed using a Windows 10 64-bit computer outfitted with an Intel Core I5 11th generation processor and 8 GB RAM. The regression model was built in Python and subsequently optimized using IGWO. The quadratic regression model was utilized for BP, whereas the cubic model was employed for thermal efficiency, BSFC, and NOx. The engine effectiveness and emission models were developed employing the following equations in the sequence of multivariate polynomial regression, as listed in Table 4.

Table 4. Multivariate polynomial regression (MPR) equations.

Parameter	Multivariate Polynomial Regression
BP (Equation (17))	$BP = -4.29312 + 14.5003X_2 + 0.00983599X_1 - 0.00754671X_1X_2 - 9.93347 \times 10^{-7}X_1^2 - 43.6933X_2^2$
BTE (Equation (18))	$BTE = -33.20698 + 122.5826X_2 - 427.2943X_2^2 + 0.07284862X_1 - 0.06358392X_1X_2 + 0.00511619X_1X_2^2 - 2.618367 \times 10^{-5}X_1^2 + 1.171184 \times 10^{-5}X_1^2X_2 + 2.798286 \times 10^{-9}X_1^3 + 780.7556X_2^3$
BSFC (Equation (19))	$BSFC = 1.2528 - 1.2505X_2 + 6.6962X_2^2 - 0.0011662X_1 + 0.00036386X_1X_2 + 8.4762 \times 10^{-5}X_1X_2^2 + 4.4791 \times 10^{-7}X_1^2 - 3.2857 \times 10^{-8}X_1^2X_2 + -5.4 \times 10^{-11}X_1^3 - 9.8667X_2^3$
NOx (Equation (19))	$NOx = 963.507143 - 158.968254X_2 - 18793.3333X_2^2 - 0.738604762X_1 + 1.02732653X_1X_2 - 1.26X_1X_2^2 + 0.0003585X_1^2 - 0.00013122449X_1^2X_2 - 5.35238095 \times 10^{-8}X_1^3 + 43777.7778X_2^3$

Note:  $X_1$  and  $X_2$  represent the engine speed and water addition percentage, respectively.

The significance of the model was determined by analysis of variance (ANOVA). The ANOVA outcomes with a 95% confidence level are displayed in Table 5. The ANOVA results indicated the significance of the estimated regression models reported in Equations (17)–(20). These results demonstrate that if the  $p$ -value is less than 0.05, the null hypothesis is rejected. If not, then the regression model can be optimized with reasonable precision.

**Table 5.** ANOVA test results of regression models.

Response	Df	f-Value	p-Value
BP	2	45.45034	0.0028
BTE	3	22.04998	0.0019
BSFC	4	5.2616	0.0026
NOx	3	1.1334	0.0069

Table 6 indicates the optimal engine speed and percentage of water addition in the W/D fuel mixture to minimize BSFC and NOx emissions while maximizing engine performance in terms of BP and BTE. The IGWO approach was used to enhance the regression models by determining the optimal input parameter values ( $x$ ). Engine speed and water addition % were the two elements that influenced these responses. First, regression models were used to estimate the responses. The IGWO technique was used to identify the optimum factor levels for these regression models. The algorithm utilizes 30 search agents with a maximum of 800 iterations to accomplish this objective. The weighted factors assigned to each variable were equal for the optimization task.

**Table 6.** Results of optimization for each response in relation to engine speed and water addition percentage.

Optimizer	Engine Speed (rpm)	Water Addition %	BP (kW)	BTE (%)	BSFC (kg/kW·h)	NOx (ppm)
GWO	1999	12%	10.7	32.8	0.274	402
IGWO	1998	9%	11.2	33.3	0.259	419

As displayed in Table 6, the fuel blend with 9% water addition had the highest BTE of 33.3%, the highest BP of 11.2 kW, the lowest BSFC of 0.259 kg/kW·h, and the lowest reduction in NOx exhaust emissions to 419 ppm at an engine speed of 1998 rpm engine speed, according to the IGWO algorithm. Compared to pure diesel, the IC engine had a BP equal to 11.259 kW at an engine speed of 2000 rpm, which is more than 0.57% compared to 9% added water and less than 1.75% for BTE. However, it achieved the highest NOx emission of 489 ppm, which is more than 14.31% of 9% water addition.

According to the GWO algorithm, the fuel blend containing 12% water has the highest BTE at 32.8%, the highest BP at 10.7 kW, the lowest BSFC at 0.274 kg/kW·h, and the lowest decrease in NOx exhaust emissions at 402 ppm. In terms of the optimizer, IGWO outperforms GWO in terms of identifying the optimal water addition and engine speed due to the fact that IGWO has strong exploration capabilities in the early stages of searching and strong exploitation capabilities in the later stages of searching. Furthermore, the wolf updating method in IGWO may reduce the chances of encountering a local optimum.

Finally, the current study was compared to others that employed W/D emulsion in CI engines, as displayed in Table 7. As displayed in Table 7, the use of a W/D emulsion fuel is an option for improving engine performance and reducing exhaust emissions from CI engines. However, most previous studies did not consider a harmonious balance between engine performance and emissions to find the optimum water addition, which has always been a significant challenge in the automotive industry. It is feasible to sacrifice a small amount of braking power to lessen the environmental effect of diesel fuel.

**Table 7.** Compare the current study to others that employed W/D emulsion in CI engines.

Ref.	CI Engine	Experimental Conditions	Water Addition	Engine Performance	Exhaust Emission	Optimal Blend
Current Study	4 Stroke, 4 Cylinder, DI, Water-cooled	FL, VS (1000–3000) rpm	0–30% Vol., 5% increment	BP ↑ until 5% BSFC ↓ until 10% BTE until 15%	NOx ↓	9% (according MPR-IGWO) 12% (according MPR-GWO)
Sharma et al., 2013 [11]	4 strokes, VCR, 661 cc, water-cooled	VL and VCR	0–25% Vol., 5% increment	BSFC ↓ and BTE ↑	CO ↓, UHC ↓, smoke ↓ and NOx ↓	10% low CR, 25% high CR
Azimi et al., 2016 [13]	4 strokes, four-cylinder, water-cooled	VS (1600–1900) rpm	0, 2, 5, 8, and 10% Vol.	PB ↓ and BT ↑	CO ↑, UHC ↓, and NOx ↓	2%
Hoseini and Sobati, 2019 [35]	4 stroke, Single cylinder, 510 CC	CS (1800 rpm), FL	0–20% Vol., 5% increment	PB ↓, BT ↓, BTE ↑, and BSFC ↑	CO ↑, UHC ↑, CO <sub>2</sub> ↑, and NOx ↓	5%
Okumş et al., 2020 [37]	4 stroke, Single cylinder, 510 CC	VS and FL	0–15% Vol., 5% increment	PB ↓, BT ↓, and BSFC ↑	NOx ↓	10%
Selim and Ghannam, 2009 [39]	4 stroke, Single cylinder,	VS, VL, VCR, and variable injection time	0–30% Vol., 5% increment	PB ↓ and BSFC ↑	-	20%
Abu Zaid, 2004 [43]	4 stroke, Single cylinder, 659 CC	FL, VS (1200–3300) rpm	0–20% Vol., 5% increment	BT ↑, PB ↑, BTE ↑, and BSFC ↓	-	20%
Kannan and Udayakumar, 2009 [53]	4 stroke, Single cylinder	CS, pressure fuel injection 200 bars	0–20% Vol., 10% increment	BSFC ↓ and BTE ↑	CO ↓, and NOx ↓	20%
Senthur et al., 2021 [54]	4 stroke, Single cylinder, 661 CC	VL	0–15% Vol., 5% increment	BTE ↑, and SFC ↑ Except 15% water addition	CO ↓, UHC ↓, smoke ↓, and NOx ↓	15%
Hassan et al., 2021 [55]	4 stroke, Single cylinder,	VL	0–10% Vol., 2% increment	BSFC ↑ and BTE ↓	CO ↑, UHC ↑, smoke ↓, and NOx ↓	10%
Khatri et al., 2021 [56]	4 stroke, Single cylinder, VCR	CS (1500 rpm)	0 and 5% Vol.	BSFC ↑ and BTE ↓	CO ↓, UHC ↓, smoke ↓, and NOx ↓	5%

VS: Variable engine speed, CS: constant engine speed, FL: Full load, VL: variable load, CR: compression ratio, VCR: variable compression ratio, ↑ increase, ↓ decrease.

## 5. Limitations, Recommendations, and Future Works

Optimization of water addition and engine speed yields substantial technical benefits, including improved engine performance, reduced environmental impacts, and lower fuel usage. Saving money and time by reducing the number of trials is another significant advantage of adopting the proposed strategy of MPR-IGOW, which optimizes mathematically modeling a system to establish the relationship between independent components. In the future, the following study limitation is examined in depth:

- For the preparation of emulsified fuel, it is desirable to have higher stability of emulsified fuel with minimum expenditure of chemicals and power so that the emulsified fuel can be used for a more extended period. In order to solve this problem, it is necessary to optimize all the factors affecting the W/D emulsion fuel, including the blending speed, stirring duration, surfactant type and concentration, oil–water ratio, temperature, pH, and hydrophilic–lipophilic balance (HLB).
- In addition to other performance factors, the optimal water content should be determined by considering the full map of environmental behavior, which includes acoustic and exhaust emissions such as noise, carbon monoxide (CO), carbon dioxide (CO<sub>2</sub>), unburned hydrocarbon (UHC), particulate matter (PM) and soot, smoke opacity, and nitrogen oxides (NOx).
- The impact of W/D emulsion fuel on fuel attributes such as flash point and cetane number, besides Fourier-transform infrared spectroscopy (FTIR). In addition, combustion parameters such as combustion gas pressure profile, P.P. increase rate, heat release rate, IDT, combustion duration, and energy and exergy analyses of the CI engine's behavior will be addressed in the forthcoming investigation.
- The effects of nanoparticle additives in W/D emulsion fuel on engine performance, exhaust emissions, and combustion behavior of a CI engine will be thoroughly examined.
- The present work suggests the following points:

- In order to avoid long-term stratification of the W/D emulsion fuel, a pump may be required to place in the bottom of a fuel tank to circulate the combination and avoid water.
- It is necessary to make adjustments to both the fuel filter and the fuel tank.

## 6. Conclusions

Identifying the optimal water addition to diesel fuel to improve engine performance and reduce emissions is a crucial challenge in the automotive industry. As a result, there must be a harmonic balance between engine performance and emissions. In some instances, surrendering some braking power to minimize the environmental effect of diesel engines is considered necessary. This study explored the impact of different water additions to diesel fuel to generate W/D emulsion fuels on diesel engine performance and NO<sub>x</sub> exhaust emissions. Furthermore, it identified the best proportion of water added and engine speed to improve the engine behavior. There, a novel framework of MPR-IGWO was proposed to find the optimum engine speed and the amount of water added. In this model, the NO<sub>x</sub> exhaust emission and BSFC were minimized, and BP and BTE were maximized by employing a multivariate polynomial regression (MPR) model incorporating IGWO. The ANOVA test was used to determine the significance of the regression models. The following points outline most experimental observations and optimization outcomes:

- The BP generated by a CI engine for various (W/D) emulsion diesel fuel ratios is highest when 5% water is added, with a 3% improvement and a slight reduction of  $-0.9%$  when 10% is added, compared to pure diesel. Because W/D emulsion fuel has a lower C.V. than pure diesel fuel, it releases less heat during combustion, which is responsible for the little drop in BP when less than 10% of water is introduced. However, a slight decrease in BP can be accepted when weighed against the enormous reduction in emissions achieved by utilizing W/D.
- The BSFC was lowest at 2000 rpm and 5% water addition. The average reduction in BSFC was  $-6.34%$  and  $-3.55%$  when utilizing 5% and 10%, respectively, compared to pure diesel. At high speed, the BSFC increased as the amount of water added to the fuel increased. However, at lower speeds, there was no substantial change in the BSFC with the quantity of additional water within the examined range.
- The maximum BTE for a CI engine was obtained with a W/D emulsion fuel ratio of 5%. The average BTE improvement was 7.94%, 5.6%, and 2.81% when water was added at levels of 5%, 10%, and 15%, respectively. Beyond this, the BTE was lower than pure diesel within the studied range as the amount of water in the emulsion increased. The improvement in BTE was due to the increased BP. Furthermore, the amount of water in the emulsion is responsible for the considerable delay in the ignition and produces latent heat during the process of vaporization. Therefore, when the ignition is delayed, which creates micro-explosions, the combustion efficiency improves dramatically.
- The CI engine generated much less NO<sub>x</sub> when the W/D emulsion fuel was utilized. The drop varied between 3.22 and 67.14%, according to the water content. This is related to the emulsion's finely distributed water droplets causing a phenomenon known as a heat sink, which reduces the temperature of an adiabatic flame.
- The viscosity of the W/D emulsion increases with the addition of water until a value of 43 centipoises at 15% water and subsequently drops. However, boosting the viscosity of W/D emulsions leads to an advanced injection time in particular injection systems.
- The MPR model and IGWO algorithms agreed well with actual experimental findings. IGWO offered optimized parameters, enhanced exploration capabilities, and a desirable computational time.
- According to the IGWO algorithm, the fuel blend with 9% water addition has the highest BTE of 33.3%, the highest BP of 11.2 kW, the lowest BSFC of 0.259 kg/kW·h, and the lowest reduction in NO<sub>x</sub> exhaust emission to 419 ppm at 1998 rpm engine speed. While according to the GWO algorithm, the fuel blend with 12% water addition has the highest BTE of 32.8%, the highest BP of 10.7 kW, the lowest BSFC of 0.274 kg/kW·h, and the lowest reduction in NO<sub>x</sub> exhaust emission to 402 ppm.

- Regarding the optimizer, the IGWO shows better results than GWO in finding the best water addition engine speed. This is because, in the early stages of searching, IGWO has strong exploration capabilities. In the later stages of searching, it has strong exploitation capabilities. Additionally, the wolf update mechanism in IGWO can lessen the likelihood of encountering the local optimum.

**Author Contributions:** Conceptualization, A.A. and H.A.; methodology, A.A., H.A. and R.A.; software, H.A. and R.A.; validation, M.A. and M.I.A.; formal analysis, H.A., A.A., M.A. and M.I.A.; investigation, H.A., A.A. and M.A.; resources, M.A. and M.I.A.; writing—original draft preparation, H.A. and A.A.; writing—review and editing, A.A., M.A. and M.I.A.; visualization, R.A.; supervision, A.A.; project administration, H.A. and A.A. All authors have read and agreed to the published version of the manuscript.

**Funding:** This research received no external funding.

**Data Availability Statement:** Not applicable.

**Acknowledgments:** The authors are grateful for the financial support offered by Tafila Technical University, Jordan.

**Conflicts of Interest:** The authors declare no conflict of interest.

## Nomenclatures

### List of Abbreviations

ABC	artificial bee colony
ANN	artificial neural network
ANOVA	analysis of variance
BP	brake power
BSFC	Brake-specific fuel consumption
BT	brake torque
BTE	brake thermal efficiency
CI	compression ignition
C.C.	combustion chamber
CO	carbon monoxide
CO <sub>2</sub>	carbon dioxide
CR	compression ratio
CS	constant engine speed
C.V.	calorific value
DC	direct current
EGR	exhaust gas recirculation
FL	Full load
GA	genetic algorithm
GWO	grey wolf optimizer
IGWO	intelligent grey wolf optimizer
IDT	ignition delay time
LL	lower limit
MAE	mean absolute error
MPR	multivariate polynomial regression
NO <sub>x</sub>	nitrogen oxides
OBL	opposition-based learning
PM	particulate matter
P.P.	peak pressure
PSO	particle swarm optimization
RME	rapeseed methyl ester

SFC	specific fuel consumption
SI	spark ignition
TDC	top dead center
UHC	unburn hydrocarbon
UL	upper limit
VCR	variable compression ratio
VL	variable load
VS	variable engine speed
W/D	water-in-diesel
WOA	whale optimization algorithm
List	of symbols
A, C	vectors
d	search space dimension
$D\alpha$ , $D\beta$ , and $D\delta$	updated location
n	polynomial degree
$r_1$ , $r_2$	random vectors
$R^2$	correlation coefficient
t	current iteration
x	a variable
X (t)	location of a wolf
$x$ , $x_1$ , $x_2$	independent variables
$X_{P(t)}$	updated position
y	dependent variable
Greek symbols	
$ \alpha $	regulate the movement of the wolf
$\omega_R$	uncertainty error
$\beta$	wolf, regression coefficient
$\omega$	realistic error, omega wolves
$\alpha$	wolf, intercept
$\delta$	wolf

## References

- Alahmer, A.; Aladayleh, W. Effect two grades of octane numbers on the performance, exhaust and acoustic emissions of spark ignition engine. *Fuel* **2016**, *180*, 80–89. [\[CrossRef\]](#)
- Zacharczuk, W.; Andruszkiewicz, A.; Tatarek, A.; Alahmer, A.; Alsaqoor, S. Effect of Ca-based additives on the capture of SO<sub>2</sub> during combustion of pulverized lignite. *Energy* **2021**, *231*, 120988. [\[CrossRef\]](#)
- Alsaqoor, S.; Alahmer, A.; Aljabarin, N.; Gougazeh, M.; Czajczynska, D.; Krzyzynska, R. Effects of utilization of solid and semi-solid organic waste using pyrolysis techniques. In Proceedings of the 2017 8th International Renewable Energy Congress (IREC), Amman, Jordan, 21–23 March 2017; pp. 1–5. [\[CrossRef\]](#)
- Khalife, E.; Tabatabaei, M.; Najafi, B.; Mirsalim, S.M.; Gharehghani, A.; Mohammadi, P.; Aghbashlo, M.; Ghaffari, A.; Khounani, Z.; Shojaei, T.R. A Novel Emulsion Fuel Containing Aqueous Nano Cerium Oxide Additive in Diesel–Biodiesel Blends to Improve Diesel Engines Performance and Reduce Exhaust Emissions: Part I—Experimental Analysis. *Fuel* **2017**, *207*, 741–750. [\[CrossRef\]](#)
- Vellaiyan, S.; Amirthagadeswaran, K.S. Emission characteristics of water-emulsified diesel fuel at optimized engine operation condition. *Pet. Sci. Technol.* **2017**, *35*, 1355–1363. [\[CrossRef\]](#)
- Alahmer, A. Influence of using emulsified diesel fuel on the performance and pollutants emitted from diesel engine. *Energy Convers. Manag.* **2013**, *73*, 361–369. [\[CrossRef\]](#)
- Scarpete, D. Diesel-Water Emulsion, an Alternative Fuel to Reduce Diesel Engine Emissions. A Review. *Mach. Technol. Mater.* **2013**, *7*, 13–16.
- Syafiq, Z.; Fahmi, O.; Awad, I.O.; Adam, A. The study of stability, combustion characteristics and performance of water in diesel emulsion fuel. *MATEC Web Conf.* **2016**, *90*, 1022. [\[CrossRef\]](#)
- Tan, Y.H.; Abdullah, M.O.; Nolasco-Hipolito, C.; Zauzi, N.S.A.; Abdullah, G.W. Engine performance and emissions characteristics of a diesel engine fueled with diesel-biodiesel-bioethanol emulsions. *Energy Convers. Manag.* **2016**, *132*, 54–64. [\[CrossRef\]](#)
- Ghojel, J.I.; Tran, X.-T. Ignition Characteristics of Diesel–Water Emulsion Sprays in a Constant-Volume Vessel: Effect of Injection Pressure and Water Content. *Energy Fuels* **2010**, *24*, 3860–3866. [\[CrossRef\]](#)
- Sharma, A.; Kumar, N.; Vibhanshu, V.; Deep, A. *Emission Studies on a VCR Engine Using Stable Diesel Water Emulsion*; SAE Technical Paper; SAE International: Warrendale, PA, USA, 2013. [\[CrossRef\]](#)
- Seifi, M.R.; Hassan-Beygi, S.R.; Ghobadian, B.; Desideri, U.; Antonelli, M. Experimental Investigation of a Diesel Engine Power, Torque and Noise Emission Using Water–Diesel Emulsions. *Fuel* **2016**, *166*, 392–399. [\[CrossRef\]](#)

13. Azimi, M.; Mirjavadi, S.S.; Davari, E.; Seifi, M.R. The effect of water-diesel emulsion usage on a tractor engine performance and emission. *Russ. Agric. Sci.* **2016**, *42*, 488–492. [[CrossRef](#)]
14. Kumar, N.; Sharma, A.; Vibhanshu, V. *Performance Analyses of Diesel Engine at Different Injection Angles Using Water Diesel Emulsion*; SAE Technical Paper; SAE International: Warrendale, PA, USA, 2013.
15. Syu, J.-Y.; Chang, Y.-Y.; Tseng, C.-H.; Yan, Y.-L.; Chang, Y.-M.; Chen, C.-C.; Lin, W.-Y. Effects of water-emulsified fuel on a diesel engine generator's thermal efficiency and exhaust. *J. Air Waste Manag. Assoc.* **2014**, *64*, 970–978. [[CrossRef](#)]
16. Ithnin, A.M.; Ahmad, M.A.; Abu Bakar, M.A.; Rajoo, S.; Yahya, W.J. Combustion performance and emission analysis of diesel engine fuelled with water-in-diesel emulsion fuel made from low-grade diesel fuel. *Energy Convers. Manag.* **2015**, *90*, 375–382. [[CrossRef](#)]
17. Attia, A.M.; Kulchitskiy, A. Influence of the structure of water-in-fuel emulsion on diesel engine performance. *Fuel* **2014**, *116*, 703–708. [[CrossRef](#)]
18. Pamminger, M.; Wang, B.; Hall, C.M.; Vojtech, R.; Wallner, T. The impact of water injection and exhaust gas recirculation on combustion and emissions in a heavy-duty compression ignition engine operated on diesel and gasoline. *Int. J. Engine Res.* **2019**, *21*, 1555–1573. [[CrossRef](#)]
19. Korakianitis, T.; Namasivayam, A.; Crookes, R. Hydrogen dual-fuelling of compression ignition engines with emulsified biodiesel as pilot fuel. *Int. J. Hydrogen Energy* **2010**, *35*, 13329–13344. [[CrossRef](#)]
20. Alahmer, H.; Alahmer, A.; Alkhazaleh, R.; Alrbai, M. Exhaust Emission Reduction of a SI Engine Using Acetone–Gasoline Fuel Blends: Modeling, Prediction, and Whale Optimization Algorithm. *Energy Rep.* **2023**, *9*, 77–86. [[CrossRef](#)]
21. Kumar, N.; Raheman, H.; Machavaram, R. Performance of a diesel engine with water emulsified diesel prepared with optimized process parameters. *Int. J. Green Energy* **2019**, *16*, 687–701. [[CrossRef](#)]
22. Khanjani, A.; Sobati, M.A. Performance and emission of a diesel engine using different water/waste fish oil (WFO) biodiesel/diesel emulsion fuels: Optimization of fuel formulation via response surface methodology (RSM). *Fuel* **2021**, *288*, 119662. [[CrossRef](#)]
23. Alahmer, A.; Rezk, H.; Aladayleh, W.; Mostafa, A.O.; Abu-Zaid, M.; Alahmer, H.; Gomaa, M.R.; Alhussan, A.A.; Ghoniem, R.M. Modeling and Optimization of a Compression Ignition Engine Fueled with Biodiesel Blends for Performance Improvement. *Mathematics* **2022**, *10*, 420. [[CrossRef](#)]
24. Alahmer, A.; Alahmer, H.; Handam, A.; Rezk, H. Environmental Assessment of a Diesel Engine Fueled with Various Biodiesel Blends: Polynomial Regression and Grey Wolf Optimization. *Sustainability* **2022**, *14*, 1367. [[CrossRef](#)]
25. Vellaiyan, S.; Amirthagadeswaran, K.S. Taguchi-Grey relational-based multi-response optimization of the water-in-diesel emulsification process. *J. Mech. Sci. Technol.* **2016**, *30*, 1399–1404. [[CrossRef](#)]
26. Lin, H.-C.; Su, C.-T.; Wang, C.-C.; Chang, B.-H.; Juang, R.-C. Parameter optimization of continuous sputtering process based on Taguchi methods, neural networks, desirability function, and genetic algorithms. *Expert Syst. Appl.* **2012**, *39*, 12918–12925. [[CrossRef](#)]
27. Ahmad, N.; Janahiraman, T.V. A Comparison on Optimization of Surface Roughness in Machining AISI 1045 Steel Using Taguchi Method, Genetic Algorithm and Particle Swarm Optimization. In Proceedings of the 2015 IEEE Conference on Systems, Process and Control (ICSPC), Bandar Sunway, Malaysia, 18–20 December 2015; pp. 129–133.
28. Alahmer, A.; Ajib, S. Solar cooling technologies: State of art and perspectives. *Energy Convers. Manag.* **2020**, *214*, 112896. [[CrossRef](#)]
29. Patil, H.; Gadhave, A.; Mane, S.; Waghmare, J. Analyzing the Stability of the Water-in-Diesel Fuel Emulsion. *J. Dispers. Sci. Technol.* **2014**, *36*, 1221–1227. [[CrossRef](#)]
30. Alahmer, A. Reduction of Particulate Matter of Diesel Emission by the Use of Several Oxygenated Diesel Blend Fuels. *Int. J. Therm. Environ. Eng.* **2014**, *7*, 45–50.
31. Mirjalili, S.; Mirjalili, S.M.; Lewis, A. Grey Wolf Optimizer. *Adv. Eng. Softw.* **2014**, *69*, 46–61. [[CrossRef](#)]
32. Saxena, A.; Soni, B.P.; Kumar, R.; Gupta, V. Intelligent Grey Wolf Optimizer—Development and application for strategic bidding in uniform price spot energy market. *Appl. Soft Comput.* **2018**, *69*, 1–13. [[CrossRef](#)]
33. Mahdavi, S.; Rahnamayan, S.; Deb, K. Opposition based learning: A literature review. *Swarm Evol. Comput.* **2018**, *39*, 1–23. [[CrossRef](#)]
34. Dryer, F. Water addition to practical combustion systems—Concepts and applications. *Symp. (Int.) Combust.* **1977**, *16*, 279–295. [[CrossRef](#)]
35. Hoseini, S.S.; Sobati, M.A. Performance and emission characteristics of a diesel engine operating on different water in diesel emulsion fuels: Optimization using response surface methodology (RSM). *Front. Energy* **2019**, *13*, 636–657. [[CrossRef](#)]
36. Alam Fahd, M.E.; Wenming, Y.; Lee, P.; Chou, S.; Yap, C.R. Experimental investigation of the performance and emission characteristics of direct injection diesel engine by water emulsion diesel under varying engine load condition. *Appl. Energy* **2013**, *102*, 1042–1049. [[CrossRef](#)]
37. Okumuş, F.; Kaya, C.; Kökkülünk, G. NOX Based Comparative Analysis of a CI Engine Fueled with Water in Diesel Emulsion. *Energy Sources Part A Recover. Util. Environ. Eff.* **2020**, 1–20. [[CrossRef](#)]
38. Nadeem, M.; Rangkuti, C.; Anuar, K.; Haq, M.; Tan, I.; Shah, S. Diesel engine performance and emission evaluation using emulsified fuels stabilized by conventional and gemini surfactants. *Fuel* **2006**, *85*, 2111–2119. [[CrossRef](#)]
39. Selim, M.Y.E.; Ghannam, M.T. Combustion Study of Stabilized Water-in-Diesel Fuel Emulsion. *Energy Sources Part A: Recover. Util. Environ. Eff.* **2009**, *32*, 256–274. [[CrossRef](#)]

40. Yang, W.; An, H.; Chou, S.; Chua, K.; Mohan, B.; Sivasankaralingam, V.; Raman, V.; Maghbouli, A.; Li, J. Impact of emulsion fuel with nano-organic additives on the performance of diesel engine. *Appl. Energy* **2013**, *112*, 1206–1212. [[CrossRef](#)]
41. Ithnin, A.M.; Noge, H.; Kadir, H.A.; Jazair, W. An overview of utilizing water-in-diesel emulsion fuel in diesel engine and its potential research study. *J. Energy Inst.* **2014**, *87*, 273–288. [[CrossRef](#)]
42. Alahmer, A.; Yamin, J.; Sakhrieh, A.; Hamdan, M. Engine performance using emulsified diesel fuel. *Energy Convers. Manag.* **2010**, *51*, 1708–1713. [[CrossRef](#)]
43. Abu-Zaid, M. Performance of single cylinder, direct injection Diesel engine using water fuel emulsions. *Energy Convers. Manag.* **2004**, *45*, 697–705. [[CrossRef](#)]
44. Vellaiyan, S.; Amirthagadeswaran, K.S. Influence of Water-in-Diesel Emulsion Fuel and Compression Ratio on Combustion, Performance and Emission Characteristics of Diesel Engine. *J. Sustain. Energy Eng.* **2016**, *3*, 238–253. [[CrossRef](#)]
45. Ghojel, J.; Honnery, D.; Al-Khaleefi, K. Performance, emissions and heat release characteristics of direct injection diesel engine operating on diesel oil emulsion. *Appl. Therm. Eng.* **2006**, *26*, 2132–2141. [[CrossRef](#)]
46. Wang, C.-H.; Chen, J.-T. An experimental investigation of the burning characteristics of water-oil emulsions. *Int. Commun. Heat Mass Transf.* **1996**, *23*, 823–834. [[CrossRef](#)]
47. Khan, M.Y.; Karim, Z.A.A.; Hagos, F.Y.; Aziz, A.R.A.; Tan, I.M. Current Trends in Water-in-Diesel Emulsion as a Fuel. *Sci. World J.* **2014**, *2014*, 527472. [[CrossRef](#)]
48. Subramanian, K. A comparison of water–diesel emulsion and timed injection of water into the intake manifold of a diesel engine for simultaneous control of NO and smoke emissions. *Energy Convers. Manag.* **2011**, *52*, 849–857. [[CrossRef](#)]
49. Basha, J.S.; Anand, R.B. An Experimental Study in a CI Engine Using Nanoadditive Blended Water–Diesel Emulsion Fuel. *Int. J. Green Energy* **2011**, *8*, 332–348. [[CrossRef](#)]
50. Jazair, W.; Kubo, S.; Takayasu, M.; Yatsufusa, T.; Kidoguchi, Y. Performance and Emission Characteristics of a Diesel Engine Fueled by Rapeseed Oil Bio-Fuel. *J. Mek.* **2011**, *33*, 32–39.
51. Selim, M.Y.E.; Elfeky, S.M.S. Effects of Diesel/Water Emulsion on Heat Flow and Thermal Loading in a Precombustion Chamber Diesel Engine. *Appl. Therm. Eng.* **2001**, *21*, 1565–1582. [[CrossRef](#)]
52. Kleinbaum, D.G.; Kupper, L.L.; Nizam, A.; Rosenberg, E.S. *Applied Regression Analysis and Other Multivariable Methods*; Cengage Learning: Boston, MA, USA, 2013; ISBN 128596375X.
53. Kannan, K.; Udayakumar, M. NO<sub>x</sub> and HC Emission Control Using Water Emulsified Diesel in Single Cylinder Diesel Engine. *ARPN J. Eng. Appl. Sci.* **2009**, *4*, 59–62.
54. Senthur, N.; BalaMurugan, S.; RamGanesh, H.; Divakara, S. Experimental analysis on the performance, emission, and combustion characteristics of diesel, and diesel-water emulsions in low heat rejection engine. *Mater. Today Proc.* **2021**, *39*, 1351–1355. [[CrossRef](#)]
55. Hassan, Z.U.; Usman, M.; Asim, M.; Kazim, A.H.; Farooq, M.; Umair, M.; Imtiaz, M.U.; Asim, S.S. Use of diesel and emulsified diesel in CI engine: A comparative analysis of engine characteristics. *Sci. Prog.* **2021**, *104*. [[CrossRef](#)]
56. Khatri, D.; Goyal, R.; Jain, A.; Johnson, A.T. Modeling and optimization of stability aspects for water diesel emulsified fuel using response surface methodology. *Energy Sources Part A: Recover. Util. Environ. Eff.* **2021**, *44*, 3055–3078. [[CrossRef](#)]

**Disclaimer/Publisher’s Note:** The statements, opinions and data contained in all publications are solely those of the individual author(s) and contributor(s) and not of MDPI and/or the editor(s). MDPI and/or the editor(s) disclaim responsibility for any injury to people or property resulting from any ideas, methods, instructions or products referred to in the content.